

BASIC RESEARCH STUDIES

The impact of model assumptions on results of computational mechanics in abdominal aortic aneurysm

Christian Reeps, MD,^a Michael Gee, PhD,^b Andreas Maier,^b Manuela Gurdan, MD,^a
Hans-Henning Eckstein, MD,^a and Wolfgang A. Wall, PhD,^b *München, Germany*

Objective: In principle, superiority of computational wall stress analyses compared with the maximum diameter criterion for rupture risk evaluation of abdominal aortic aneurysm (AAA) has been demonstrated. The results of finite element analyses should be evaluated carefully, however, because computational strains and stresses are highly dependent on the quality and complexity of each step of AAA simulation. Most clinically active vascular specialists are not familiar with the processes of computational mechanics to evaluate the quality of AAA simulations. For better understanding and to provide insights in computational biomechanics of AAA, the effect of different computational model assumptions on the results of simulation are explained and demonstrated.

Methods: Four patients with asymptomatic ($n = 3$) and symptomatic ($n = 1$) infrarenal AAAs with distinctly different aneurysm morphologies were exemplarily studied. For segmentation and 3-dimensional (3D) reconstruction of AAA and thrombus, 3-mm computed tomography (CT) slices were used, and a high-density hexahedral element-dominated finite element mesh was generated. Subsequent AAAs were simulated on seven different levels, culminating in the most realistic ortho-pressure-finite element analyses simulations, including thrombus, wall calcifications, and prestress state of AAA geometry with nonlinear hyperelastic material and geometric model assumptions.

Results: Alterations in displacements due to model assumptions are up to 740% for a specific aneurysm. The average maximum discrepancy among the four morphologies between simple and advanced models is 607%. Differences in peak wall stress between simple and realistic models are up to 210% individually and 170% on average.

Conclusion: Differences of model assumptions are more important for simulation results than differences between patient-specific morphologies. Because the biomechanical behavior of AAA is nonlinear in many senses, comparisons between individual morphologies and statistics are only valid when detailed information about preconditions and model assumptions is provided. (*J Vasc Surg* 2010;51:679-88.)

Clinical Relevance: The potentially improved accuracy in rupture risk stratification of abdominal aortic aneurysms (AAA) by individualized computational simulations is attractive for physicians, scientists, and patients. However, the results of finite element model simulations are highly dependent on the quality and complexity of the underlying finite element models. As a consequence, interpretation of results in many publications is difficult and the results are often not comparable. Unfortunately, most clinically active vascular specialists are not familiar with computational analyses of AAA to evaluate the quality of such studies. For better understanding and to provide insights in computational AAA biomechanics, the effects of more and less sophisticated model assumptions are explained and demonstrated in four exemplary AAA morphologies.

From the Department of Vascular Surgery, Klinikum rechts der Isar,^a and the Institute for Computational Mechanics,^b Technische Universität München.

This work received support from the International Graduate School of Science and Engineering of the Technische Universität München, Germany, under Project 2-11 and 3-7.

Competition of interest: none.

Reprint requests: Christian Reeps, MD, Abteilung für Gefäßchirurgie, Klinikum rechts der Isar der Technischen Universität München, Ismaninger Str 22, 81675 München, Germany (e-mail: christian.reeps@arcor.de).

The editors and reviewers of this article have no relevant financial relationships to disclose per the JVS policy that requires reviewers to decline review of any manuscript for which they may have a competition of interest.

0741-5214/\$36.00

Copyright © 2010 by the Society for Vascular Surgery.

doi:10.1016/j.jvs.2009.10.048

Rupture of abdominal aortic aneurysm (AAA) is the 13th leading cause of death in Western societies and is fatal in 70% to 90%. In consequence, the precise prediction of AAA rupture risk is essential. With the current, well-established computed tomography (CT) morphologic parameters, such as maximum aortic diameter, aneurysm shape, and AAA expansion, only the relative—but not the individual—rupture risk can be determined.¹ Trusting in the commonly used and highly evidence-based maximum diameter criterion presents uncertainties, however, because AAA rupture may occur unexpectedly in small aneurysms that are below the critical diameter limits,^{2,3} whereas many large aneurysms may remain stable throughout patient's lifetime⁴ without the potential harm of prophylactic surgery.

Table I. Patient and abdominal aortic aneurysm characteristics

<i>Patient</i>	<i>Age (y)</i>	<i>AAA diameter (mm)</i>	<i>Symptoms</i>	<i>Morphology</i>	<i>Calcification^a</i>
Male40	71	45	–	Sacciform	Medium
Female59	48	54	–	Fusiforme	Slight
Male42	66	48	–	Fusiforme	Severe
Male39	68	87	+	Fusiforme	Slight

–, Asymptomatic; +, symptomatic; AAA, abdominal aortic aneurysm.

^aAneurysm wall calcifications.

A more precise prediction of AAA rupture risk is essential. The main determinants of AAA formation and rupture are biomechanical forces exerted by blood pressure and the strength of the withstanding aortic wall. Although the evaluation of individual patient-specific AAA wall stability in vivo presently remains unsolved, individually acting wall stresses can be calculated more and more precisely by computational methods.⁵⁻⁷ In contrast to the established plain maximum diameter criterion, the finite element method (FEM) used in computational simulations of AAA is based on patient-specific AAA morphology, material properties of the AAA wall, and load by blood pressure forces.

In principle, the superiority of these computational wall stress analyses compared with the maximum diameter criterion for rupture risk evaluation of AAA has been demonstrated by several studies,⁸⁻¹⁰ and the potentially improved accuracy in risk stratification of AAA is attractive for physicians, scientists, and patients. A deluge of reports dealing with computational simulations has been published.⁵ The results of commonly used and less sophisticated FEM simulations should be evaluated very carefully, however, because the resulting computational strains and stresses are highly dependent on the quality and complexity of the underlying finite element models¹¹ and the preconditions of the simulation as accuracy of 3-dimensional (3D) AAA reconstruction, meshing, and the number and type of finite elements used. The way blood pressure load is modelled, the material law used for the AAA wall, the inclusion or omission of intraluminal thrombus (ILT), and wall calcification and the prestress state of individual AAA geometry are also essential for the results of AAA simulations.

As a consequence in most publications, interpretation of results is difficult and the results often are not comparable. Unfortunately, most clinically active vascular specialists are not familiar with the processes of computational mechanics and its potentials and limitations to evaluate quality of AAA simulations. For better understanding and to provide insights in computational biomechanics of AAA, the effect of different model assumptions on the results of quasistatic simulation is demonstrated exemplarily by analyses of four patient-specific AAA morphologies.

METHODS

All image and data analyses were performed retrospectively and anonymously and were therefore exempted from the approval of our Institutional Review Board.

Patients. Four patients (1 woman, 3 men) with asymptomatic (n = 3) or symptomatic (n = 1) infrarenal AAA and different aneurysm morphologies underwent CT scans as part of elective or emergency evaluation and were included retrospectively in this analysis. All patients underwent open AAA repair immediately after CT imaging based on the recommendations of our in-hospital vascular board for different indications. For the asymptomatic woman (Female59), indication was given by maximum infrarenal cross-sectional diameter (maxdia = 54 mm). Of the three male patients, one with a fusiform asymptomatic and heavily calcified AAA (maxdia = 48 mm) had surgery on his own preference, another with an asymptomatic small AAA (maxdia = 45 mm) had surgery due to sacciform AAA morphology, and one with a large symptomatic AAA (maxdia = 87 mm) had emergency repair. Morphologic characteristics are summarized in Table I.

Imaging and segmentation. All retrospectively analyzed CT data sets were obtained from a Philips Brilliance 64 channel CT Scanner (Philips Healthcare, DA Best, The Netherlands) and performed as contrast-enhanced thoracoabdominal multislice CT angiography with the intravenous injection of 100 mL contrast medium (Imeron 300, Byk-Gulden, Konstanz, Germany), table speed of 12 mm/s, with bolus tracking and a collimation of 64 × 0.6 mm. Primary data sets were reconstructed in 0.6- and 3.0-mm slices.

For preparation of FEM analyses, the 3-mm CT DICOM data slices were converted using Mimics 12.01 postprocessing software (Materialize, Leuven, Belgium) for semiautomatic segmentation and 3D reconstruction of the AAA lumen by thresholding, region growing algorithms, and manual corrections. In addition, direct 3D segmentation of ILT is performed rather than centerline-oriented segmentation techniques. Luminal thrombus geometry is reconstructed accurately, but the AAA wall itself cannot be detected from the CT data⁸⁻¹² and therefore is assumed to have a 1-mm uniform thickness extruded from the outer ILT surface throughout all models. Hexahedral element-dominated finite element meshes with the highest computational and mechanical reliability are generated with a basic mesh size of 1.0 mm (Fig 1) by using Harpoon commercial software (Sharc Ltd, Manchester, UK). The number of finite elements and connecting nodes for each patient-specific computational AAA model are depicted in Table II.



Fig 1. Horizontal cut through a three-dimensional reconstructed abdominal aortic aneurysm (*Female59*) prepared for simulation demonstrates computational grid density of the aneurysm wall and the intraluminal thrombus.

Table II. Basic preconditions of abdominal aortic aneurysm simulation

Patient	No. of elements ^a		No. of nodes ^a	
	With ILT	Without ILT	With ILT	Without ILT
Male40	72.899	5.883	40.033	8.451
Female59	594.798	30.550	385.847	44.500
Male42	625.406	122.598	369.036	116.808
Male39	1.100.130	52.367	586.700	74.744

ILT, Intraluminal thrombus.

^aNumber of finite elements and mesh nodes used for simulation for each patient-specific AAA morphology studied with and without intraluminal thrombus.

AAA modelling

Subsequent to mesh generation, the four AAAs are simulated using seven different levels of model complexity, model 1 through model 7. Model assumptions are chosen with respect to selected assumptions of geometry, material,

and mechanical behavior and are combined and altered from uncomplicated and simple to complex and most realistic to demonstrate the influence of individual assumptions and their interplay. With increasing model number, a more advanced and sophisticated combination of model assumptions is applied, as summarized in Table III and detailed in the following. Spatially constant systolic blood pressure of 120 mm Hg is applied to achieve comparability among individual AAAs, and quasistatic structural analyses have been performed in all cases, neglecting the influence of fluid-structure interaction.

Geometric modeling. The 3D morphologies of AAAs obtained from in vivo CT scans are processed as previously described. Here, we discuss the effect of explicit consideration of intraluminal thrombus on the results. In model 1 through model 4, patient-specific thrombus is neglected (NoILT); in model 5 through model 7, thrombus is explicitly considered (ILT). Furthermore, the effect of wall calcifications (ILT_wCalc) on strains, stresses, and deformations is demonstrated (ILT_wCalc) in one AAA (Male42).^{13,14}

Material modeling. To demonstrate the impact of arterial wall material assumptions on the results of AAA simulations, we compared a simple, isotropic linear elastic material model (LinMat)¹⁵ with a realistic nonlinear hyperelastic material (NonLinMat) model based on experimental data of mechanical AAA wall tests.¹⁶

For the LinMat material, a Young's modulus of $E = 1.044 \times 10^6$ Pa and a Poisson ratio of $\nu = 0.49$ [–] is assumed, where E represents the stiffness and ν reflects the almost incompressible behavior typical for soft tissue.

For the NonLinMat material, $\alpha = 1.74 \times 10^5$ Pa, $\beta = 1.881 \times 10^6$ Pa, and $\nu = 0.49$ [–] are applied,¹⁶ where $\alpha = E/6$ refers to the initial stiffness and β reflects the hardening behavior in the large strain regimen.

Both material models (LinMat and NonLinMat) are isotropic, meaning that the strain-stress relationship is identical in longitudinal and circumferential direction. Although this assumption is invalid for healthy anisotropic aortic wall, it is more realistic in fibrotic AAA wall material.¹⁷ Further intraluminal thrombus is taken into account (ILT or ILT_wCalc). ILT material is modelled as a nearly incompressible isotropic hyperelastic neo-Hookean material ($E = 1.044 \times 10^5$ Pa, $\nu = 0.45$ [–]).^{18,19} However, these ILT material properties^{18,19} are averaged values, even though thrombus content, density, relative compaction, and friability may vary substantially in vivo. Calcifications are also modelled as isotropic hyperelastic neo-Hookean material but with significantly higher stiffness ($E = 5.0 \times 10^7$ Pa and $\nu = 0.4$ [–]).

All AAA aortic wall material parameters were taken from previous data,¹⁶ and calcification parameters are based on mechanical testing of human AAA material that we performed previously. Consideration of calcifications in simulation was done, as recently published.¹³

Mechanical modeling. In vivo, at any point in time of the cardiac cycle, blood pressure, forces of inertia, and stresses within AAA wall and ILT are in balance (equilib-

Table III. Combination of methods, materials, and model assumptions in abdominal aortic aneurysm simulation^a

Model	Material law	Equilibrium	Ortho-pressure	Prestressing	ILT	Time ^b
1	Linear	Linear	34
2	Linear	Nonlinear	1951
3	Linear	Nonlinear	Yes	1875
4	Nonlinear	Nonlinear	Yes	1443
5	Nonlinear	Nonlinear	Yes	...	Yes	11470
6	Nonlinear	Nonlinear	Yes	Yes	Yes	14318
7	Nonlinear	Nonlinear	Yes	Yes	Yes (calc)	...

Calc, Aneurysm wall calcifications; *ILT*, intraluminal thrombus.

^aIncreasing complexity of abdominal aortic aneurysm (AAA) simulation from model 1 to 7 based on combinations of material and modeling assumptions and methods named, as described in Methods.

^bTotal computing time in seconds needed on a 8-processor AMD-Opteron cluster (2.6 GHz) using the software “baci” exemplary for Female59 abdominal aortic aneurysm.

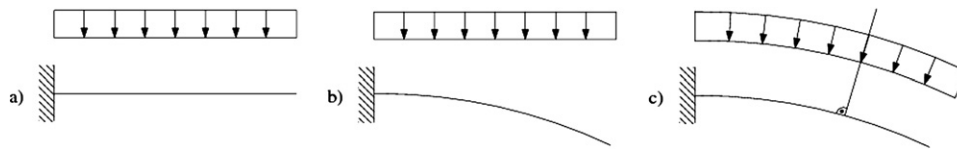


Fig 2. An exemplary illustration shows equilibrium and blood pressure load using a simple cantilever beam. Equilibrium and load are shown (a) with respect to the known reference geometry obtained from imaging (LinGeom and NonOrthPressure) and (b) with respect to the unknown deformed geometry. The pressure load is shown with respect to the reference geometry (NonLinGeom and NonOrthPressure). (c) Equilibrium and true pressure load are shown with respect to the unknown deformed geometry (NonLinGeom and OrthPressure).

rium). In simulation, this balance of forces is sought by the finite element analysis with respect to a specific geometric configuration of the AAA. Two choices of configuration are feasible: The first is that balance is sought with respect to a known geometric configuration, which is the geometry obtained from imaging. Because the geometry is known, the equations of equilibrium are independent of the deformation and turn out to be linear (LinGeom model). This leads to a greatly reduced computational effort.

The second and much more realistic choice is to seek equilibrium of forces with respect to the deforming AAA configuration at the snapshot in time that is being investigated. In this case, the equilibrium is sought with respect to the true current configuration (that is not yet determined), and the equilibrium therefore depends on this unknown configuration (NonLinGeom model). Mechanical details of LinGeom and NonLinGeom equations have been previously published.^{20,21} The equations of equilibrium are nonlinear, yielding a significantly increased computational cost.

For ease of understanding we illustrate this discussion by means of an exemplary toy problem in Fig 2: in panel A, equilibrium is sought with respect to an known undeformed configuration (LinGeom); in panel B, equilibrium is sought with respect to a deformed configuration which is part of the problem solution itself (NonLinGeom), and panel C, illustrates one choice in methodology of applying blood pressure load that is discussed in the following.

Forces exerted by blood pressure can be modelled orthogonal to the initial undeformed lumen surface (Fig 2, A).

For the deformed AAA, the applied pressure is no longer orthogonal to the deformed luminal surface nor does it match the increased luminal surface area (NonOrthPressure). More realistically, the direction of the applied blood pressure is always perpendicular (orthogonal) to the surface of the deforming geometry (OrthoPressure; Fig 2, C). Blood pressure is applied to the lumen surface when ILT or ILTwCalc is used and to the arterial wall directly in the NoILT case.

Prestressing. The in vivo AAA geometry displayed by CT imaging is at least under diastolic pressure and therefore represents a deformed geometry with matching stress and strain state already contained. In simple simulations, this fact is neglected completely or only the pressure difference between diastolic and systolic blood pressure is considered.²² For rupture risk, however, evaluation of the total amount of stress is relevant. Another coarse but simple and commonly used model assumption is to take the initial AAA geometry as stress-free and apply total systolic blood pressure to it, termed here the NoPreStress model.

In contrast, strains and stresses present in AAA geometry at the time of imaging can be considered by computational prestressing (PreStress model) techniques.²³⁻²⁷ Therein, a certain pressure level, for example, constant diastolic blood pressure of 80 mm Hg, is considered to be already contained in the geometry configuration at time of imaging, and the corresponding strain/stress state is computed in an inverse analysis. The pressure difference from diastolic to systolic level can be applied in a following step, yielding a

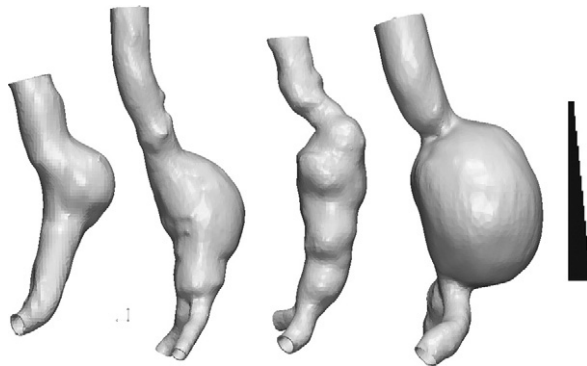


Fig 3. Analyzed abdominal aortic aneurysms (AAA) with exemplarily different morphology. **Left to right**, Sacciform (Male40), fusiforme (Female59), fusiform (Male42), and large fusiforme symptomatic AAA (Male39).

realistic AAA deformation and total stress state as detailed by Gee et al.²³

Boundary conditions. Computational simulations require appropriate boundary conditions applied to the region of interest. Although the choice of such boundary conditions in hemodynamic flow and fluid-structure interaction simulations is very complex and crucial for the obtained results, it is usually sufficient in quasi-static stress analyses to clamp all ends of the artery section under investigation as long as the boundary is reasonably far away from the aneurysm. Other choices of computational boundary conditions also are conceivable.

Simulations were performed on an eight-processor high-performance computing system using our inhouse finite element software “baci.” Exemplary timings for individual models applied to the Female59 AAA are supplied in Table III. Model 1 is very efficient due to the purely linear nature of the assumptions. Models 2 through 4 require comparable computational effort. The inclusion of ILT material greatly increases the overall problem size that results in models 5 through 7 consuming significantly more time. Consideration of the prestressing stress state (model 6 and 7) adds some additional cost to the calculations due to the prestressing algorithm.

RESULTS

The four selected AAAs (Fig 3) were studied under six different combinations of geometry, material, and mechanical assumptions (models 1 through 6) that were described in detail Methods and are listed in Table III. In addition, model 7, which explicitly considers calcification, was applied to the Male42 AAA with severe calcifications of AAA wall. Fig 1 displays a horizontal cut through the mesh of the Female59 AAA, visualizing mesh density and 3D geometry of lumen, ILT, and assumed aortic wall. For comparability, all results were obtained under an assumed systolic blood pressure of 120 mm Hg, whereas in model 6 and model 7 prestressing was considered as described in Methods, and it was assumed that a constant diastolic pressure of 80 mm

Table IV. Results of variant abdominal aortic aneurysm simulation for maximum displacement (mm)

AAA	AAA simulation model ^a						
	1	2	3	4	5	6	7
Male40	13.4	5.8	9.8	5.8	4.9	1.1	...
Female59	16.7	6.61	1.9	6.4	6.2	1.4	...
Male42	36.0	7.9	12.2	7.3	6.0	1.2	0.8
Male39	54.0	15.7	28.6	13.5	12.9	2.1	...

AAA, Abdominal aortic aneurysm.

^aSimulation models 1 through 7 are described in Table III and in Methods.

Hg was present at the time of imaging. Results of computed maximum peak wall stresses and maximum AAA displacements are provided in Tables III and IV and are visualized in Figs 4 through 7, respectively.

Model 1. In this most simple simulation, the resulting maximum peak wall stresses and maximum displacements are excessively high, with unrealistic ballooning and out-pouching of the in vivo geometry (maximum displacements from 1.3 to 5.5 cm) under systolic blood pressure load. This clearly is unrealistic to an extent that invalidates simulations performed using modelling assumptions combined in model 1 (Table I). We investigated this model for the sake of completeness.

Model 2. In contrast to model 1, the modelling of equilibrium is modified from LinGeom to NonLinGeom as previously described. By this modification, computed maximum displacement and peak wall stresses (PWS) in all simulated AAA are reduced to still high but much more realistic levels. Peak wall stresses are reduced to 1% to 8% and maximum displacement of AAA to 23% to 43% compared with model 1.

Model 3. Compared with model 2, internal pressure loads are changed from NonOrthoPressure to nonlinear OrthoPressure modelling conditions, resulting in higher peak wall stresses.

Model 4. Here a nonlinear material model¹⁶ specially designed for AAA and derived from experimental testing is introduced into simulation (NonLinMat). Nonlinear material modelling thereby leads to markedly decreased PWS and displacement DP in all AAA with highest consequence in large AAA owing to the nonlinear stiffening of the material in the regime of large strains.

Model 5. In addition to model 4, model 5 explicitly considers ILT geometry. Depending on thrombus amount, thickness, and grade of eccentricity of the AAA, considering thrombus is highly relevant for simulation and results in reduced maximum PWS (20% to 48%) and noticeably diminished maximum wall displacements (3% to 16%) in the four analyzed AAA. The highest relative cushion effect is seen for the small but very eccentric AAA (Male40) in which ILT filled nearly the entire AAA sack cavity. In contrast to the Male40 AAA, the cushion effect of the thin thrombus lining in the large symptomatic AAA (Male39) is clearly lower. Explicit consideration of thrombus material reduces the lumen surface and therefore the area upon

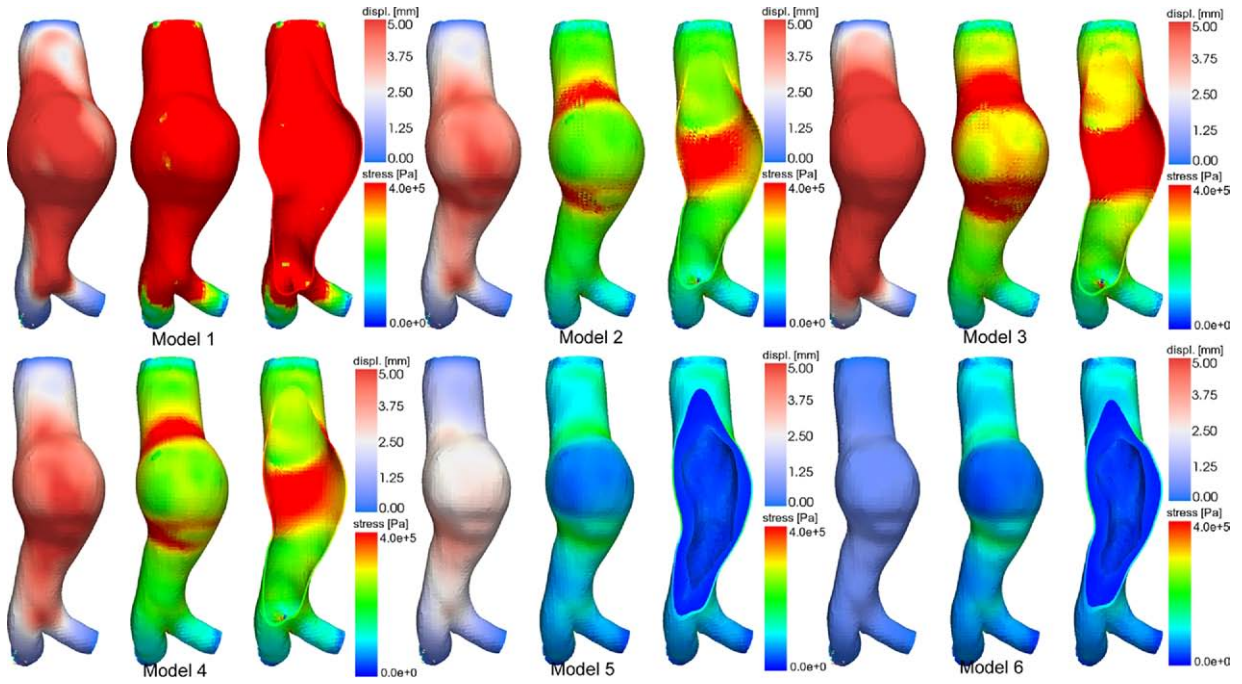


Fig 4. Simulation results for models 1 to 6 for the Male40 abdominal aortic aneurysm (AAA), as described in Table III and in Methods. **Left,** Color indicates deformation in mm. **Center,** Color indicates wall stress (von Mises stress; Pa). **Right,** Coronal cut through AAA where color indicates wall stress (von Mises stress; Pa).

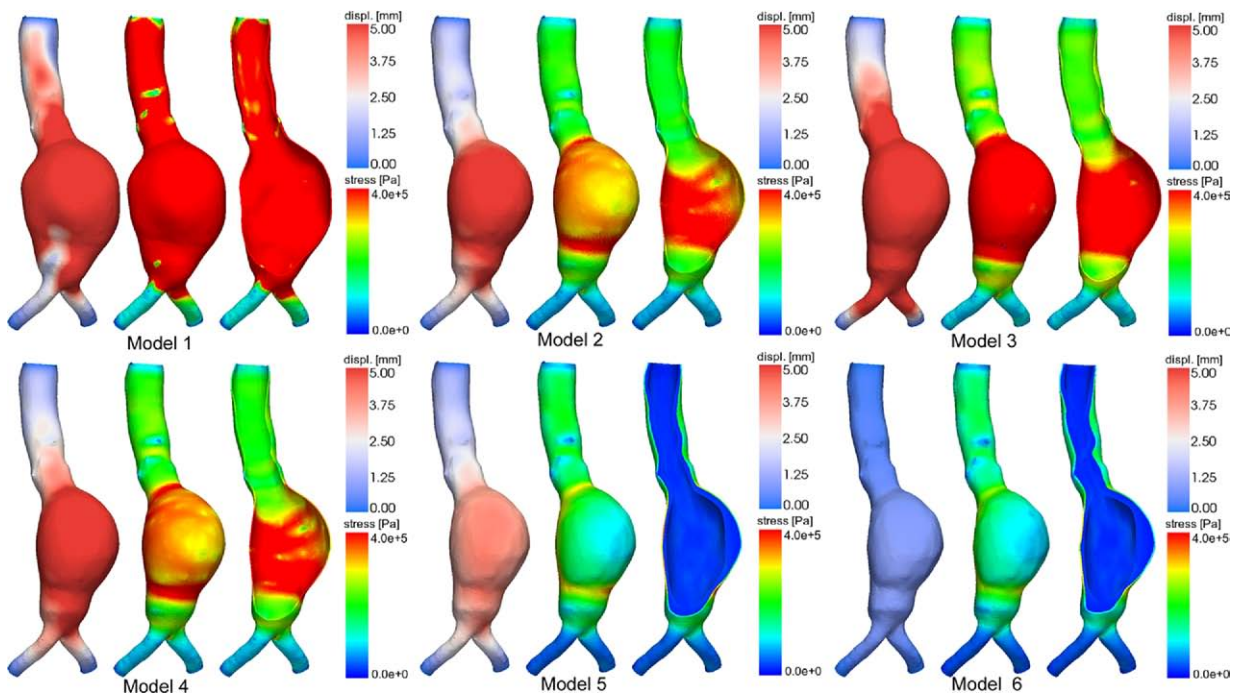


Fig 5. Simulation results for models 1 to 6 for the Female59 abdominal aortic aneurysm, as described in Table III and in Methods. **Left,** Color indicates deformation in mm. **Center,** Color indicates wall stress (von Mises stress; Pa). **Right,** Coronal cut through AAA where color indicates wall stress (von Mises stress; Pa).

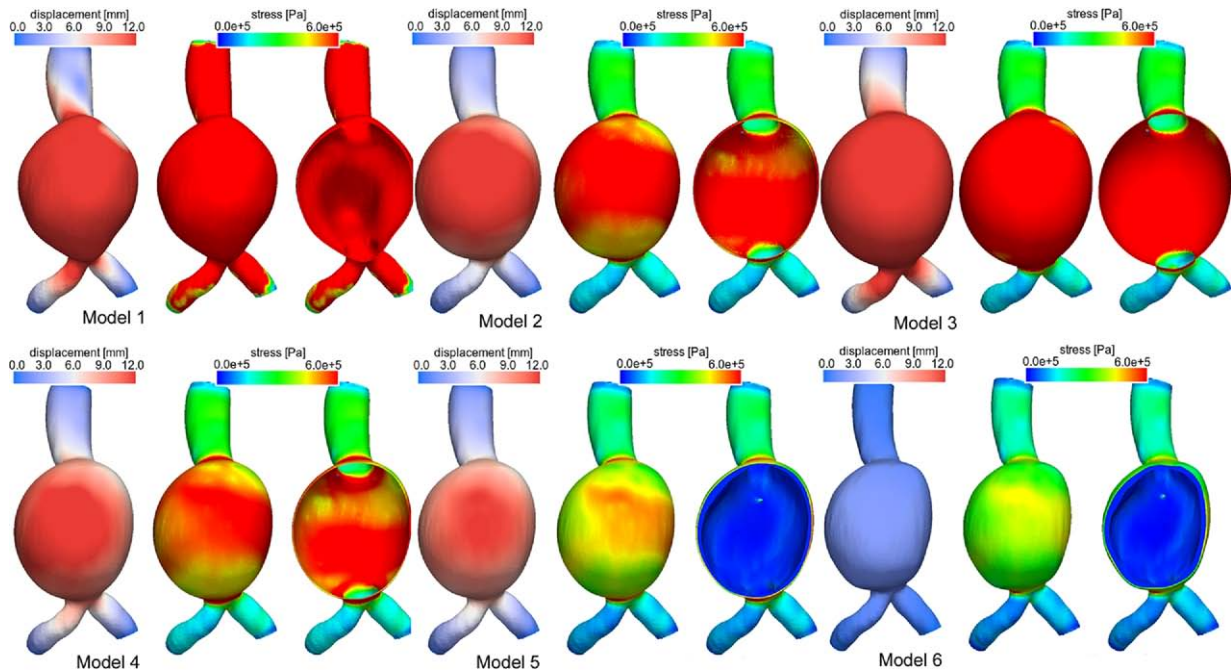


Fig 6. Simulation results for models 1 to 6 for the Male39 abdominal aortic aneurysm (AAA), as described in Table III and in Methods. **Left,** Color indicates deformation in mm. **Center,** Color indicates wall stress (von Mises stress; Pa). **Right,** Coronal cut through AAA where color indicates wall stress (von Mises stress; Pa).

which blood pressure acts. Consequently, the integral amount of load subjected to the structure is diminished.

Model 6. In model 6 compared with model 5, prestressing of the initial AAA geometry up to 80 mm Hg is performed as previously described. Prestressing of the AAA structure in particular leads to a decrease of AAA deformation to realistic levels as observed in vivo. Maximum AAA wall displacements are reduced approximately 80% compared with model 5 and yield a realistic 1.05 to 2.1 mm with strong correlation to maximum AAA diameter. Moreover, prestressing results in decreased PWS in the AAA wall by 11% to 17%.

Model 7. This model was studied in one patient (Male42) with severe atherosclerotic lesions the influence of intramural calcifications on calculated PWS and displacement. Calcifications attract stresses resulting in decreased stresses in the arterial wall itself, whereas stress peaks may occur at the edges of calcifications. Overall, calcifications do not influence PWS dramatically but diminish displacements. Although spatial stress distribution patterns are similar in models 1 through 6, calcifications also strongly influence spatial distribution of stresses. Interestingly, indentations of the Male42 AAA morphology are congruent to areas with higher calcifications, whereas adjacent areas show a significant out-pouching.^{2,28} This can be taken as an indicator that calcifications significantly affect the remodelling and growth processes within the AAA wall.

DISCUSSION

Computed wall stresses, strains, and deformation by finite element analyses are a promising approach in the prediction of patient-specific AAA rupture risk. In AAA biomechanics with the help of computer simulations, sophisticated numeric models are needed to determine the influence of the appearing loads on the aortic wall and ILT in its entire complexity. Finite element analysis techniques have been validated experimentally²⁹ and numerically³⁰ in idealized AAA models in principal and have demonstrated superiority in the prediction of AAA rupture risk compared with the clinically established maximum diameter criterion.^{9,31}

However, stresses and strains represent only the influence of mechanical loads on the AAA, whereas the ability of the aortic wall to resist is opposed. If stress and strains are close to or higher than resistance of the aneurysm wall at first, compensatory remodelling of AAA wall occurs and later, rupture.³²

Inherently, thickness, nonlinear material behavior, strength of the AAA wall, and the spatial distribution of these quantities are essential for the accuracy of AAA simulation results and therefore a realistic prediction of AAA rupture risk. So far, however, no imaging technique exists that preoperatively offers information on material properties of an individual AAA wall. Hence, it is even more important to model the biomechanical behavior of AAAs as accurately as possible with respect to known quantities, such as ILT geometry, and model assumptions, such as

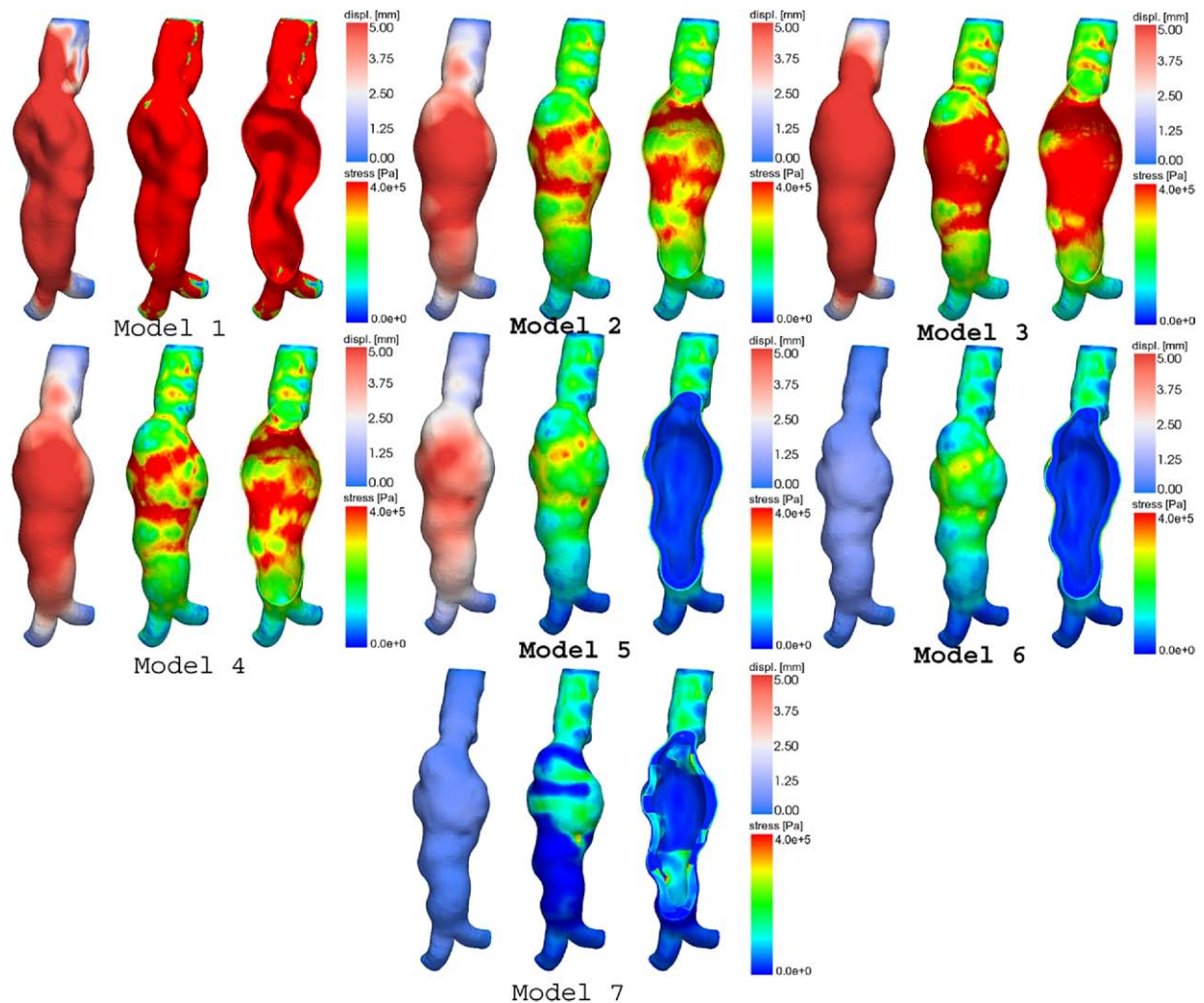


Fig 7. Simulation results for models 1 to 7 for the Male42 abdominal aortic aneurysm (AAA) as described in Table III and in Methods. **Left,** Color indicates deformation in mm. **Center,** Color indicates wall stress (von Mises stress; Pa). **Right,** Coronal cut through AAA where color indicates wall stress (von Mises stress; Pa).

prestressing, that are preoperatively available and represent state of the art modelling techniques.

Assumptions made due to the unavailability of information are a uniform thickness of 1 mm of the arterial wall and a uniform spatial distribution of the material properties, as was described. Also, for ease of discussion, no effects due to remodeling,^{33,34} anisotropy,³⁵ and fluid-structure interaction^{22,36,37} are considered here. Thereby, the contribution of fluid-structure interaction to total wall stress is negligible compared with the influence of overall blood pressure level.²⁸ Moreover, the influence of segmentation quality on results is well known¹¹ and therefore was excluded from this discussion.

Major differences due to model assumptions are found regarding the maximum displacements more than for PWS levels. For all simulations with models 1 through 5, displacements are high with unrealistic ballooning of AAA

geometry, even if thrombus is explicitly considered (model 5). Immoderate deformations are the consequence if AAA geometry at the time of imaging is regarded as stress free. Only models 6 and 7, which use the described prestressing technique, decreased maximum displacements by 78% to 84% and evinced physiologically meaningful deformations of approximately 1 to 2 mm (Table IV; Figs 4-7, respectively). These findings are in good accordance with visual observations of diameter expansion during the cardiac cycle in open AAA repair.

PWS levels, in contrast, are reduced uniformly by 11% to 17% when prestressing is used. Consequently, considering prestressing is important in studies concerning rupture risk. In addition to maximum deformation analyses, PWS levels vary significantly throughout the rather simple models 1 through 4. These simple models with nonlinear geometrical modelling, ortho-pressure simulation, nonlinear

Table V. Results of variant abdominal aortic aneurysm simulation for maximum peak wall von Mises stress (kPa)

AAA	AAA simulation model ^a						
	1	2	3	4	5	6	7
Male40	7200	460	620	480	250	220	...
Female59	6400	520	820	540	420	350	...
Male42	16000	540	760	560	360	320	220 (520 in calc)
Male39	68000	840	2300	700	560	480	...

AAA, Abdominal aortic aneurysm; *calc*, calcification.

^aSimulation models 1 through 7 are described in Table III and in the Methods.

material properties, but neglecting ILT and prestressing, achieve PWS levels not exceeding the physiologic thresholds of maximum human AAA wall strength of about 800 kPa derived from ex vivo mechanical testing¹⁶ but fail to allow for quantitative assessment of rupture risk analysis because PWS is significantly overestimated (Table V).

Furthermore, the nonlinearity inherent to AAA simulation leads to unforeseeable changes of maximum patient-specific PWS levels, and the choice of modelling assumptions leads to results that can vary significantly more among deferring model assumptions applied to the same AAA morphology than between individual patient-specific morphologies with identical computational models. Appropriate mechanical, material, and geometric models therefore have to be considered essential in any patient-specific study of statistical relevance because it potentially can shift results of studies significantly and also alters comparison between individual morphologies due to the nonlinear mechanical nature. However, the application of model 2 already results in very high computational expenses when sufficiently fine computational meshes are used and, for example, cannot be computed on a personal computer.

CONCLUSIONS

Varying model assumptions influence results to a larger extent than the difference between patient-specific morphologies. Alterations in displacements due to the different model assumptions are up to 740% for a specific aneurysm, even when neglecting the most trivial model 1. The average maximum discrepancy among the four morphologies between the simple model 2 and model 6 is 607%. Differences in peak wall stress between model 2 and model 6 are up to 210% individually and average 170%. Therefore, as the biomechanical behavior of AAA is nonlinear in multiple senses, comparisons between individual morphologies and statistics based on patient-specific case studies are only valid when sufficient model complexity is applied. Good assessment of computational models applied in case studies is crucial for realistic simulation results and reliable rupture risk prediction and should be performed as collaborative work among medical and engineering researchers.

AUTHOR CONTRIBUTIONS

Conception and design: CR, MG

Analysis and interpretation: CR, MG, AM, MG

Data collection: CR, MG, AM, MG

Writing the article: CR, MG

Critical revision of the article: AM, MG, WW, HE

Final approval of the article: AM, MG, WW, HE

Statistical analysis: Not applicable

Obtained funding: WW, HE

Overall responsibility: WW

HE and WW contributed equally to this work.

REFERENCES

- Brewster JH, Cronenwett JL, Johnston K, Krupski W, Matsumura J. Guidelines for the treatment of abdominal aortic aneurysms. *J Vasc Surg* 2003;37:1106-17.
- Darling R, Messina C, Ottinger D. Autopsy study of unoperated abdominal aortic aneurysms. The case for early resection. *Circulation* 1977;56:161-4.
- Nicholls S, Gardner J, Meissner M, Johansen H. Rupture in small abdominal aortic aneurysms. *J Vasc Surg* 1998;28:884-8.
- Ashton H, Buxton M, Day N, Kim L, Marteau T, Scott R. The multicentre aneurysm screening study (mass) into the effect of abdominal aortic aneurysm screening on mortality in men: a randomised controlled trial. *Lancet* 2002;360:1531-9.
- Humphrey J, Taylor C. Intracranial and abdominal aortic aneurysms: Similarities, differences, and need for a new class of computational models. *Ann Rev Biomed Eng* 2008;10:221-46.
- Vorp D. Biomechanics of abdominal aortic aneurysms. *J Biomech* 2007;40:1887-902.
- Lasheras J. The biomechanics of arterial aneurysms. *Ann Rev Fluid Mech* 2007;39:293-319.
- Fillinger M, Raghavan M, Marra S, Croonenwett J, Kennedy F. In vivo analysis of mechanical wall stress and abdominal aortic aneurysm rupture risk. *J Vasc Surg* 2002;36:589-97.
- Fillinger M, Marra S, Raghavan M, Kennedy F. Prediction of rupture risk in abdominal aortic aneurysm during observation: wall stress versus diameter. *J Vasc Surg* 2003;37:724-32.
- Raghavan M, Fillinger M, Marra S, Naegle B, Kennedy F. Automated methodology for determination of stress distribution in human abdominal aortic aneurysm. *J Biomech Eng* 2005;127:868-71.
- Doyle B, Callanan A, McGloughlin T. A comparison of modelling techniques for computing wall stress in abdominal aortic aneurysms. *BioMed Eng Online* 2007;6:38.
- Vorp D, Raghavan M, Webster M. Mechanical wall stress in abdominal aortic aneurysm: influence of diameter and asymmetry. *J Vasc Surg* 1998;27:632-9.
- Maier A, Gee MW, Reeps C, Eckstein HH, Wall WA. Explicit treatment of calcifications in patient specific stress analyses of abdominal aortic aneurysm. *J Biomech* [in press].
- Speelman L, Bohra A, Bosboom E, Schurink G, van de Vosse F, Makaroun M, et al. Effects of calcifications in patient-specific wall stress analyses of abdominal aortic aneurysms. *J Biomech Eng* 2007;129:105-9.
- Holzappel GA. *Nonlinear solid mechanics*. New York: Wiley Press; 2000.
- Raghavan M, Vorp D. Toward a biomechanical tool to evaluate rupture potential of abdominal aortic aneurysm: identification of a finite strain

- constitutive model and evaluation of its applicability. *J Biomech* 2000;33:475-82.
17. Raghavan M, Webster MW, Vorp D. Ex vivo biomechanical behavior of abdominal aortic aneurysm: assessment using a new mathematical model. *Ann Biomed Eng* 1996;24:573-82.
 18. Wang DHJ, Makaroun MS, Webster MW, Vorp DA. Effect of intraluminal thrombus on wall stress in patient-specific models of abdominal aortic aneurysm. *J Vasc Surg* 2002;36:598-604.
 19. Vande Geest JP, Sacks MS, Vorp DA. A planar biaxial constitutive relation for the luminal layer of intra-luminal thrombus in abdominal aortic aneurysms. *J Biomech* 2006;39:2347-54.
 20. Hughes TJR. The finite element method: linear static and dynamic finite analysis. New York: Prentice Hall; 1987.
 21. Crisfield M. Non-linear finite element analysis of solids and structures. New York: John Wiley & Sons, 1997.
 22. Martino ED, Guadagni G, Fumero A, Ballerini G, Spirito R, Biglioli P, et al. Fluid-structure interaction within realistic 3D models of the aneurysmatic aorta as a guidance to assess the risk of rupture of the aneurysm. *Med Eng Phys* 2001;23:647-55.
 23. Gee M, Reeps C, Eckstein H, Wall W. Prestressing in finite deformation abdominal aortic aneurysm simulation. *J Biomech* 2009;42:1732-9.
 24. Gee M, Förster C, Wall W. A computational strategy for prestressing patient-specific biomechanical problems under finite deformation. *Comm Numeric Methods Eng Biomed Appl* [published online DOI 10.1002/cnn.1236].
 25. Fachinotti V, Cardona A, Jetteur P. Finite element modelling of inverse design problems in large deformation anisotropic hyperelasticity. *Int J Numeric Methods Eng* 2008;74:894-910.
 26. Lu J, Zhou X, Raghavan M. Inverse elastostatic stress analysis in pre-deformed biological structures: demonstration using abdominal aortic aneurysms. *J Biomech* 2007;40:693-6.
 27. Lu J, Zhou X, Raghavan M. Inverse method of stress analysis for cerebral aneurysms. *J Biomech Model Mechanobiol* 2008;7:477-86.
 28. Leung HL, Wright AR, Cheshire N, Crane J, Thom SA, Hughes AD, et al. Fluid structure interaction of patient specific abdominal aortic aneurysms: a comparison with solid stress models. *BioMedical Engineering Online* 5 2006;33:1-15.
 29. Morris L, O'Donnell P, Delassus P, McGloughlin T. Experimental assessment of stress patterns in abdominal aortic aneurysms using the photoelastic method. *Strain* 2004;40:165-72.
 30. Callanan A, Morris L, McGloughlin T. Numerical and experimental analysis of an idealised abdominal aortic aneurysm. Presented at: European Society of Biomechanics S-Hertogenbosch, Netherlands; 2004.
 31. Heng MS, Fagan MJ, Collier JW, Desai G, McCollum PT, Chetter IC. Peak wall stress measurement in elective and acute abdominal aortic aneurysms. *J Vasc Surg* 2008;47:17-22.
 32. Choke E, Cockerill G, Wilson WR, Sayed S, Dawson J, Loftus I, et al. A review of biological factors implicated in abdominal aortic aneurysm rupture. *Eur J Vasc Endovasc Surg* 2005;30:227-44.
 33. Figueroa C, Bæk S, Taylor C, Humphrey J. A computational framework for coupled fluid-solid growth in cardiovascular simulations. *Comput Method Appl Mech Eng* [in press].
 34. Volokh K, Vorp D. A model of growth and rupture of abdominal aortic aneurysm. *J Biomech* 2008;41:1015-21.
 35. Geest JV, Sacks M, Vorp D. The effects of aneurysm on the biaxial mechanical behavior of human abdominal aorta. *J Biomech* 2006;39:1324-34.
 36. Figueroa C, Vignon-Clementel I, Jansen K, Hughes T, Taylor C. A coupled momentum method for modelling blood flow in three-dimensional deformable arteries. *Comput Method Appl Mech Eng* 2006;195:5685-706.
 37. Rissland P, Alemu Y, Einav S, Ricotta J, Bluestein D. Abdominal aortic aneurysm risk of rupture: patient-specific FSI simulations using anisotropic model. *J Biomech Eng* 2009;131:031001.

Submitted May 25, 2009; accepted Oct 4, 2009.